Rab35 regulates cadherin-mediated adherens junction formation and myoblast fusion

Sophie Charrasse[a], Franck Comunale[a], Sylvain De Rossi[b], Arnaud Echard[c], and Cécile Gauthier-Rouvière[a]

[a]Centre de Recherche de Biochimie Macromoléculaire, Universités Montpellier 2 et 1, Centre National de la Recherche Scientifique, Unité Mixte de Recherche 5237, 34293 Montpellier, France; [b]Montpellier RIO Imaging, BioCampus Montpellier, 34094 Montpellier, France; [c]Membrane Traffic and Cell Division Laboratory, Institut Pasteur, Centre National de la Recherche Scientifique, URA2582, 75015 Paris, France

ABSTRACT **Cadherins are homophilic cell–cell adhesion molecules implicated in many fundamental processes, such as morphogenesis, cell growth, and differentiation. They accumulate at cell–cell contact sites and assemble into large macromolecular complexes named adherens junctions (AJs). Cadherin targeting and function are regulated by various cellular processes, many players of which remain to be uncovered. Here we identify the small GTPase Rab35 as a new regulator of cadherin trafficking and stabilization at cell–cell contacts in C2C12 myoblasts and HeLa cells. We find that Rab35 accumulates at cell–cell contacts in a cadherin-dependent manner. Knockdown of *Rab35* or expression of a dominant-negative form of Rab35 impaired N- and M-cadherin recruitment to cell–cell contacts, their stabilization at the plasma membrane, and association with p120 catenin and led to their accumulation in transferrin-, clathrin-, and AP-2–positive intracellular vesicles. We also find that Rab35 function is required for PIP5KIγ accumulation at cell–cell contacts and phosphatidyl inositol 4,5-bisphosphate production, which is involved in cadherin stabilization at contact sites. Finally, we show that Rab35 regulates myoblast fusion, a major cellular process under the control of cadherin-dependent signaling. Taken together, these results reveal that Rab35 regulates cadherin-dependent AJ formation and myoblast fusion.**

Monitoring Editor
Kozo Kaibuchi
Nagoya University

Received: Feb 28, 2012
Revised: Nov 5, 2012
Accepted: Nov 20, 2012

INTRODUCTION

Cadherins are highly conserved transmembrane receptors that mediate calcium-dependent cell–cell adhesion and form adherens junctions. They play essential roles during embryonic development by regulating cell differentiation, growth, and migration and in the maintenance of tissue architecture in adult life (Takeichi, 1995; Halbleib and Nelson, 2006; Harris and Tepass, 2011). Perturbation of cadherin function is associated with cancer cell invasion and metastasis (Christofori, 2003). Cadherins mediate homotypic cell–cell adhesion through their extracellular domain (Troyanovsky, 2005), whereas their cytoplasmic domains interact with a range of proteins that link cadherins to the cytoskeleton and to cell signaling pathways (Kemler, 1993; Perez-Moreno *et al.*, 2003).

Formation of cell–cell contacts is a multistep process that includes cadherin association with catenins, delivery of cadherin–catenin complexes to the plasma membrane (PM), lateral diffusion in the PM toward cell–cell contact sites, cadherin oligomerization, homotypic interactions, and association of cadherin complexes with their intracellular partners and the actin cytoskeleton. Moreover, cadherin-based cell–cell contacts are dynamic adhesive structures, and the trafficking and turnover of cadherins to and from the PM play an important role in this dynamic behavior (Yap *et al.*, 2007; Schill and Anderson, 2009; Baum and Georgiou, 2011). Much attention has been focused on the role of the Rho and Arf families of small GTPases in cadherin-dependent adhesion (Braga *et al.*, 2000; Fukata and Kaibuchi, 2001; Palacios *et al.*, 2001; Lozano *et al.*, 2003), whereas the implication of the Rab family of small GTPases that includes >60 proteins is much less known. Rab GTPases define specific trafficking routes within the secretory and endocytic pathways by controlling several transport steps, such as vesicle formation, motility, docking, and fusion (Zerial and McBride,

This article was published online ahead of print in MBoC in Press (http://www.molbiolcell.org/cgi/doi/10.1091/mbc.E12-02-0167) on November 28, 2012.

Address correspondence to: Cécile Gauthier-Rouvière (cecile.gauthier@crbm.cnrs.fr).

Abbreviations used: AJ, adherens junction; $PI(4,5)P_2$, phosphatidyl inositol 4,5-bisphosphate; PM, plasma membrane.

2001; Stenmark, 2009). In particular, Rab11 has been involved in E-cadherin recycling and apical membrane formation in mammals and *Drosophila* (Desclozeaux *et al.*, 2008; Roeth *et al.*, 2009), Rab5 and Rab7 in lysosomal targeting of E-cadherin in Src-induced epithelial-to-mesenchymal transition (Palacios *et al.*, 2005), and Rab5 and Rab11 in N-cadherin trafficking during neuronal migration (Kawauchi *et al.*, 2010). To determine whether some Rab family members might play a role in cadherin-dependent adhesion, we analyzed their localization and found that Rab35 strongly accumulated at cell–cell contacts. Rab35 is ubiquitously expressed and localizes at the PM and in endocytic compartments and controls a fast endocytic recycling pathway (Kouranti *et al.*, 2006; Patino-Lopez *et al.*, 2008). Rab35 has been also involved in cytokinesis, phagocytosis, and neurite outgrowth (Kouranti *et al.*, 2006; Chevallier *et al.*, 2009; Dambournet *et al.*, 2011; Egami *et al.*, 2011; Kobayashi and Fukuda, 2012). Moreover, several types of cargo, such as T-cell and major histocompatibility class I (MHCI) receptors, KCa2.3 Ca^{2+}-activated K^+ channels, and the oocyte receptor in *Caenorhabditis elegans*, require Rab35 for their recycling (Patino-Lopez *et al.*, 2008; Allaire *et al.*, 2010; Gao *et al.*, 2010). In addition to its role in the regulation of membrane trafficking, Rab35 modulates actin organization directly through its effectors, by controlling Rac1 and Cdc42 localization at the PM, or through Arf6 (Zhang *et al.*, 2009; Shim *et al.*, 2010; Dambournet *et al.*, 2011; Egami *et al.*, 2011; Kobayashi and Fukuda, 2012).

Here we show that Rab35 is recruited to cell–cell contacts in a cadherin-dependent manner. *Rab35* knockdown dramatically affects N-, M-, and E-cadherin recruitment to cell–cell contacts and the PM and leads to accumulation of cadherins in intracellular vesicles in both myoblasts and HeLa cells. Absence of Rab35 activity decreases the accumulation of phosphatidyl inositol 4,5-bisphosphate ($PI(4,5)P_2$) and PIP5KIγ at cell–cell contacts, a change that also participates in the loss of cadherins at these sites. We thus identify Rab35 as a new regulator of adherens junction (AJ) formation.

RESULTS

Rab35 localizes at cell–cell contacts and associates with cadherin complexes

To investigate the possible involvement of Rab family members in cadherin-dependent adhesion, we expressed wild-type Rab4, Rab5, Rab7, Rab8, Rab11, and Rab35 fused to green fluorescent protein (GFP) in C2C12 mouse myoblasts and HeLa cells and then monitored their localization and that of N- and M-cadherin. In both cell lines, only Rab35 accumulated at cell–cell contact sites, where it colocalized with N- and M-cadherin (Figure 1, A and B, for myoblasts; Supplemental Figure S1, A and B, for HeLa cells).

Moreover, cadherins triggered Rab35 recruitment to cell–cell contact sites. Indeed, in mouse L cells, which do not express endogenous cadherins, Rab35 did not accumulate at cell contacts. Conversely, upon expression of exogenous N-, M-, or E-cadherin, Rab35 was recruited to cell contacts, where it colocalized with the expressed cadherin (Figure 1C). This is specific for Rab35, because none of the other tested Rab family members (Rab4, Rab5, Rab7, and Rab11) was recruited to cell–cell contacts in a cadherin-dependent manner (Supplemental Figure S1C).

Finally, in immunoprecipitation experiments using anti–N- or -M-cadherin antibodies and whole-cell extracts of C2C12 myoblasts and HeLa cells that express wild-type Rab35 (Rab35WT) fused to GFP, Rab35 was immunoprecipitated together with endogenous N-cadherin (Figure 1D, a and c) or M-cadherin (Figure 1Db), as revealed by Western blot analysis. Similarly, endogenous Rab35 was immunoprecipitated together with M-cadherin in C2C12 myoblasts (Supplemental Figure S1D). Rab11 was not found in the M-cadherin complex, whereas the Rab35 effector fascin was.

These findings show that Rab35 is complexed with N- and M-cadherin and colocalizes with these cadherins at cell contact sites. They also indicate that Rab35 recruitment at cell–cell contacts is induced by cadherins.

Rab35 is involved in AJ formation

To get insights into Rab35 function at cell–cell contact sites, we generated by retroviral infection stable C2C12 cell lines in which *Rab35* expression was inactivated by RNA interference. Two *Rab35* short hairpin RNAs (shRNAs; *Rab35* shRNA1 and *Rab35* shRNA2) were used to generate a pool (Figure 2A) and various cell clones that were selected using a resistance marker (Supplemental Figure S2, A and B). As controls, parental and C2C12 myoblasts expressing a luciferase shRNA (*Luci* shRNA) were used (Fortier *et al.*, 2008). We first investigated whether Rab35 inactivation influenced N- and M-cadherin localization. In parental and *Luci* shRNA C2C12 myoblasts, N- and M-cadherin accumulated at cell–cell contacts (Figure 2B, a and b and g and h, respectively; arrows). In contrast, their accumulation at cell–cell contacts was perturbed in *Rab35* shRNA C2C12 myoblasts (Figure 2B, c–f and i–l, arrowheads), whereas their intracellular localization increased (Figure 3). We confirmed this result by expressing a dominant-negative mutant of Rab35 (Rab35S22N) in C2C12 myoblasts (Supplemental Figure S2C). Again, N- and M-cadherin localization at cell–cell contacts was disrupted in 60% of C2C12 and HeLa cells expressing Rab35S22N (Supplemental Figures S2C and S3 and Supplemental Videos S1–S4). Moreover, cadherins accumulated in intracellular vacuoles (asterisks in Supplemental Figure S2C and Supplemental Figures S4 and S5) that were induced by Rab35S22N expression, as previously shown for other cargoes (Kouranti *et al.*, 2006; Patino-Lopez *et al.*, 2008; Chesneau *et al.*, 2012). Thus cadherin localization at cell–cell contacts was perturbed in *Rab35*-knockdown cells and upon expression of Rab35S22N.

Of importance, we did not detect any significant difference in the total expression levels of N- and M-cadherin in cells expressing *Rab35* shRNA1 and 2 in comparison to parental and control *Luci* shRNA C2C12 myoblasts (Figure 2C). To further quantify N- and M-cadherin levels at the cell surface of *Luci* shRNA and *Rab35* shRNA C2C12 myoblasts, we used a cell surface biotinylation assay (Figure 2D). Quantification of the results showed that *Rab35* knockdown decreased the amount of both N- and M-cadherin at the PM. Because cadherin stability at cell–cell contacts is dependent on the binding of p120 catenin (Davis *et al.*, 2003; Xiao *et al.*, 2003), we then analyzed whether *Rab35* silencing decreased p120 catenin association with N- and M-cadherin. Although the level of p120 catenin was not modified in *Rab35* shRNA C2C12 myoblasts (Figure 2Ea), p120 catenin association with N-cadherin (Figure 2Eb) and M-cadherin (Figure 2Ec) was significantly decreased. In contrast, the association of β-catenin with M-cadherin was not modified in *Rab35* shRNA C2C12 myoblasts.

Moreover, the reduced accumulation of cadherins at the PM of *Rab35* shRNA C2C12 myoblasts was accompanied by increased N- and M-cadherin accumulation in transferrin-labeled recycling compartments (Figure 3A). Similar results were obtained upon Rab35S22N expression (Supplemental Figure S5). Accumulation of N- and M-cadherin in transferrin-labeled recycling compartments was even higher when cell–cell contact disruption induced by Rab35S22N was enhanced by ethylene glycol tetraacetic acid (EGTA) treatment (Supplemental Figure S5). As previously described (Rahajeng *et al.*, 2012), functional inhibition of *Rab35* led to

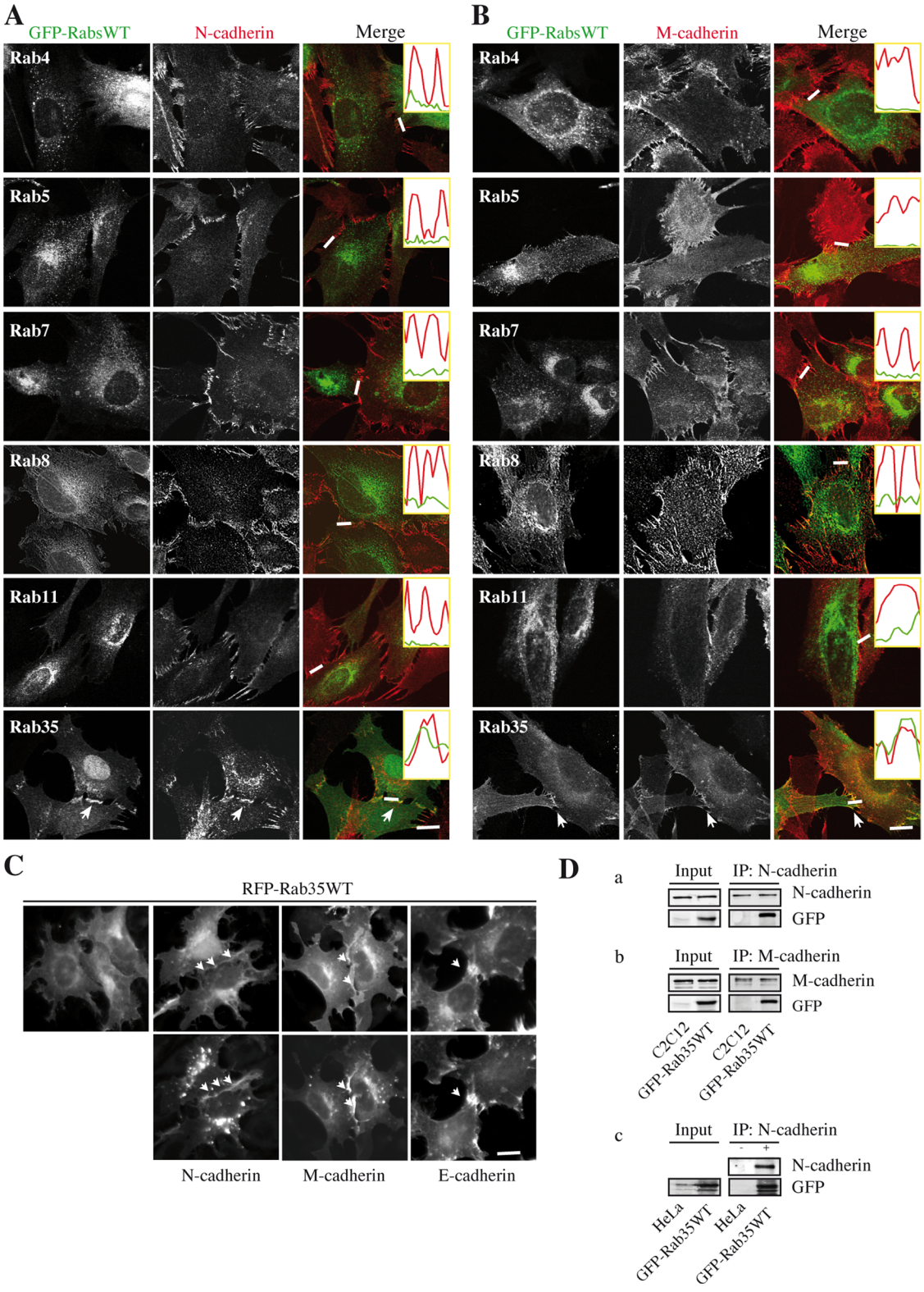

FIGURE 1: Rab35 colocalizes and is complexed with N- and M-cadherin at cell–cell contacts. (A, B) C2C12 myoblasts were transfected with GFP-tagged Rab4, Rab5, Rab7, Rab8, Rab11, and Rab35, stained for N-cadherin (A) or M-cadherin (B) expression, and analyzed by confocal microscopy. Arrows show colocalization of cadherins and GFP-Rab35 at cell contact sites. Quantification of the two signals was performed along the white line shown in the "merge" panels by line scan (MetaMorph software). Bar, 10 μm. (C) Mouse L cells that express plasmids encoding either RFP-Rab35WT alone or with N-, M-, or E-cadherin/GFP. Arrows show cadherins and Rab35 accumulation at cell–cell contacts. Bar, 10 μm. (D) Cell lysates from control and GFP-Rab35WT-transfected C2C12 myoblasts (a, b) and HeLa cells (c) were immunoprecipitated using anti–N- or M-cadherin (+) or an irrelevant (–) antibodies and immunoblotted to assess the presence of cadherins and GFP-Rab35.

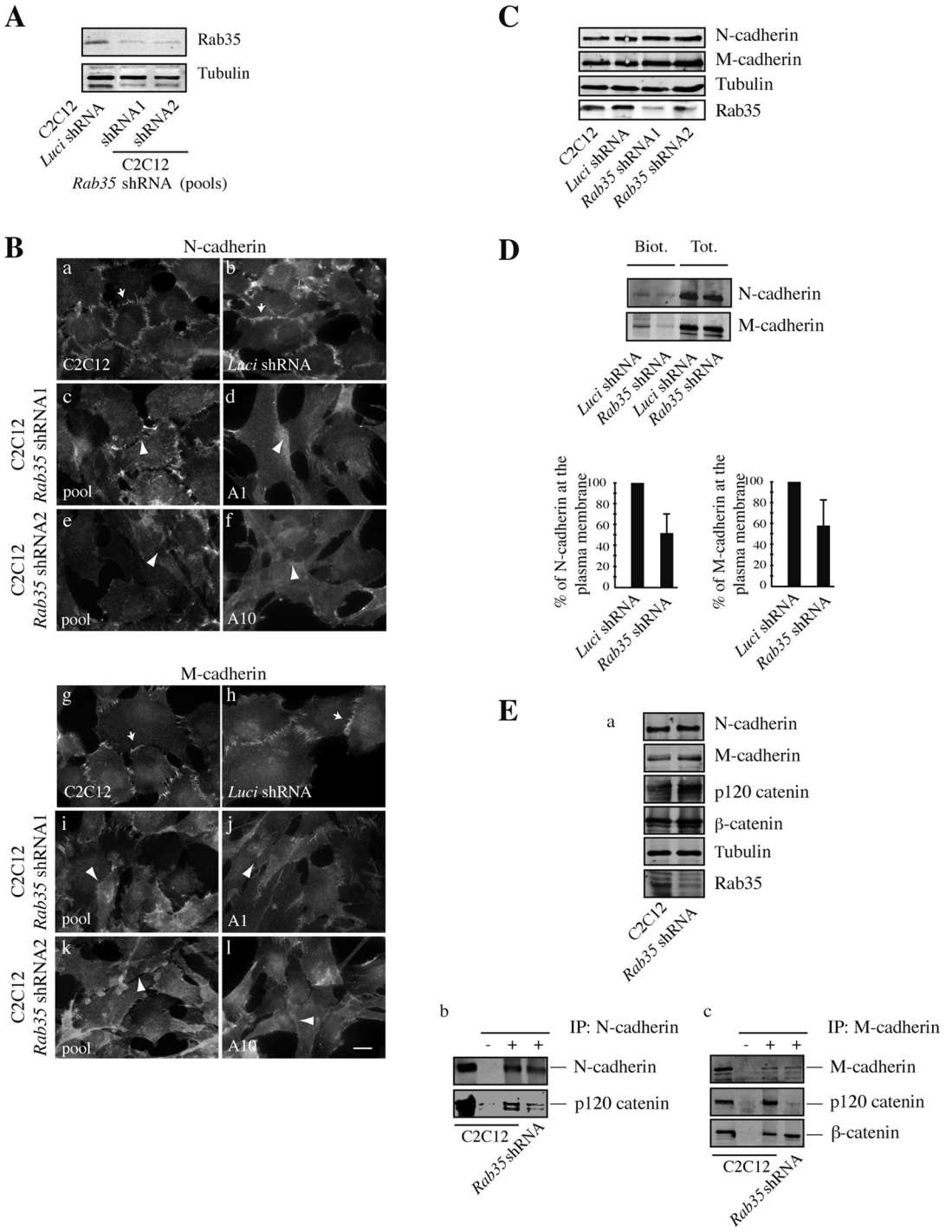

FIGURE 2: Rab35 is required for N- and M-cadherin accumulation at cell–cell contacts. (A) Cell lysates (30 µg) of control *Luci* shRNA and *Rab35* shRNA C2C12 myoblasts were assessed by Western blot analysis for expression of Rab35 and α-tubulin. (B) N- and M-cadherin localization was analyzed by indirect immunofluorescence in parental and *Luci* shRNA (controls; a and b, and g and h), *Rab35* shRNA1 C2C12 myoblasts (c and d, and i and j) and *Rab35* shRNA2 C2C12 myoblasts (e and f, and k and l). Arrows show cadherin accumulation at cell contact sites, and arrowheads show absence of cadherin accumulation at cell contact sites. Bar, 10 µm. (C) Cell lysates (30 µg) of parental, *Luci* shRNA, and *Rab35* shRNA C2C12 myoblasts cultured in growth medium (GM) were assessed by Western blot analysis for expression of N-cadherin, M-cadherin, tubulin, and Rab35. (D) *Luci* shRNA (control) and *Rab35* shRNA C2C12 myoblasts were cell surface biotinylated at 4°C. Biotinylated N- and M-cadherin were recovered onto streptavidin beads. The N- and M-cadherin contents in total and biotinylated fractions were analyzed by immunoblotting. The histogram represents the quantification of biotinylated cadherins at the PM normalized to the total amount of cadherins calculated from at least three independent experiments. (E) a, Expression of N- and M-cadherin, p120 and β-catenin, α-tubulin, and Rab35 was analyzed by Western blotting in cell lysates from parental (control) and *Rab35* shRNA C2C12 myoblasts. b, c, Cell lysates of control and *Rab35* shRNA C2C12 myoblasts were immunoprecipitated using anti–N-cadherin (b) or anti–M-cadherin (c) antibodies and probed for the presence of p120 and β-catenin. (–) Control immunoprecipitations were performed using irrelevant immunoglobulins G.

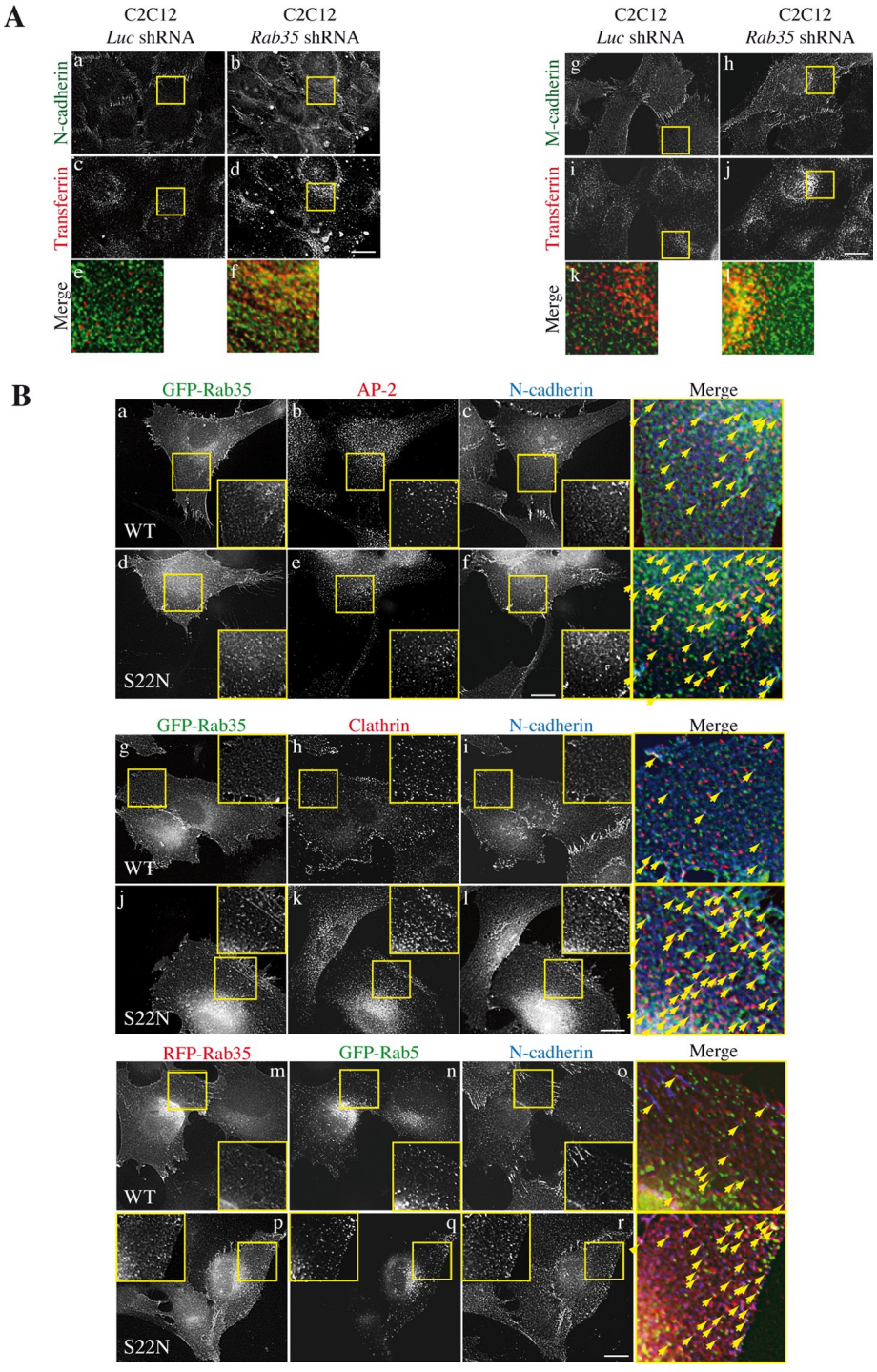

FIGURE 3: Rab35 is required for N- and M-cadherin delivery and stabilization at the PM. (A) *Luci* shRNA (control) and *Rab35* shRNA C2C12 myoblasts were incubated with rhodamine-labeled transferrin at 37°C for 45 min and stained for N- or M-cadherin. Images were acquired using a wide-field microscope and deconvolved using the Huygens system image restoration software. Distribution of N-cadherin (a and b), M-cadherin (g and h), transferrin alone (c and d, and i and j), or merge with N-cadherin (e and f) or M-cadherin (k and l). Selected areas in e, f, k, and l are shown enlarged under the merged images. Bar, 10 μm. (B) C2C12 myoblasts were transfected with GFP-tagged Rab35WT or Rab35S22N and stained for N-cadherin and AP-2 (a–f) or N-cadherin and clathrin heavy chain expression (g–l). C2C12 myoblasts were cotransfected with RFP-tagged Rab35WT or Rab35S22N and GFP-tagged Rab5 and N-cadherin expression assessed (m–r). Images were acquired using a wide-field microscope and deconvolved using the Huygens system image restoration software. Selected areas are shown enlarged as insets in each panel and the colocalization of the three proteins in the selected area in the merged images. Bar, 10 μm.

accumulation of transferrin in the perinuclear region (Figure 3A, d and j). These N- or M-cadherin–containing endocytic vesicles were positive for AP-2, clathrin, and to a lesser extent Rab5 (Figure 3B) but not for other endocytic markers, such as EEA1, Rab4, and Rab11 (unpublished data). Accumulation of N- or M-cadherin in AP-2–, clathrin-, and Rab5-positive vesicles was higher in C2C12 myoblasts that express Rab35S22N than in cells expressing Rab35WT (Figure 3B).

Taken together, these data show that *Rab35* silencing does not affect the total expression level of N- and M-cadherin but perturbs their localization at the PM and their stabilization at cell–cell contacts.

Rab35 controls PI(4,5)P_2 accumulation at cell–cell contact sites

We previously demonstrated PI(4,5)P_2 accumulation and colocalization with N- and M-cadherin at cell contacts in C2C12 myoblasts (Taulet *et al.*, 2009; Bach et al., 2010). Given that Rab35 regulates the localization of PI(4,5)P_2 at the PM (Kouranti *et al.*, 2006), we then assessed whether *Rab35* knockdown affected its accumulation and colocalization with N-cadherin in C2C12 myoblasts. To this aim, we transfected parental and *Rab35* shRNA C2C12 myoblasts with a construct that expresses the PH domain of PLCδ fused to GFP (PH-PLCδ-GFP) that specifically binds to PI(4,5)P_2 (Varnai and Balla, 1998). PI(4,5)P_2 accumulated at the PM and at cell–cell contacts in control cells (Figure 4Aa, arrow) but not in *Rab35* shRNA C2C12 myoblasts (Figure 4Ac, arrowhead). To confirm that Rab35 regulates PI(4,5)P_2 accumulation at cell contacts, we analyzed the localization of PH-PLCδ-GFP during cell–cell contact reformation upon Ca^{2+} recovery after chelation with EGTA. *Rab35* knockdown affected PI(4,5)P_2 accumulation at cell–cell contacts also after Ca^{2+} recovery (Figure 4A, compare b and d). Specifically, whereas 70% of cell–cell contacts showed PI(4,5)P_2 enrichment in control cells, this dropped to 30% in *Rab35* shRNA C2C12 myoblasts. Expression of the Rab35 dominant-negative mutant Rab35S22N in C2C12 myoblasts also reduced PI(4,5)P_2 accumulation at cell–cell contacts (Figure 4B). In contrast, no perturbation of PI(4,5)P_2 localization at cell–cell contacts was observed after expression of Rab35WT or Rab35Q67L, a constitutively active form of Rab35. Moreover, both Rab35 isoforms colocalized with PI(4,5)P_2 at cell–cell contacts (Figure 4B). We also analyzed PI(4,5)P_2 levels at cell–cell contacts using an antibody that specifically detects this phosphoinositide. To perform a more

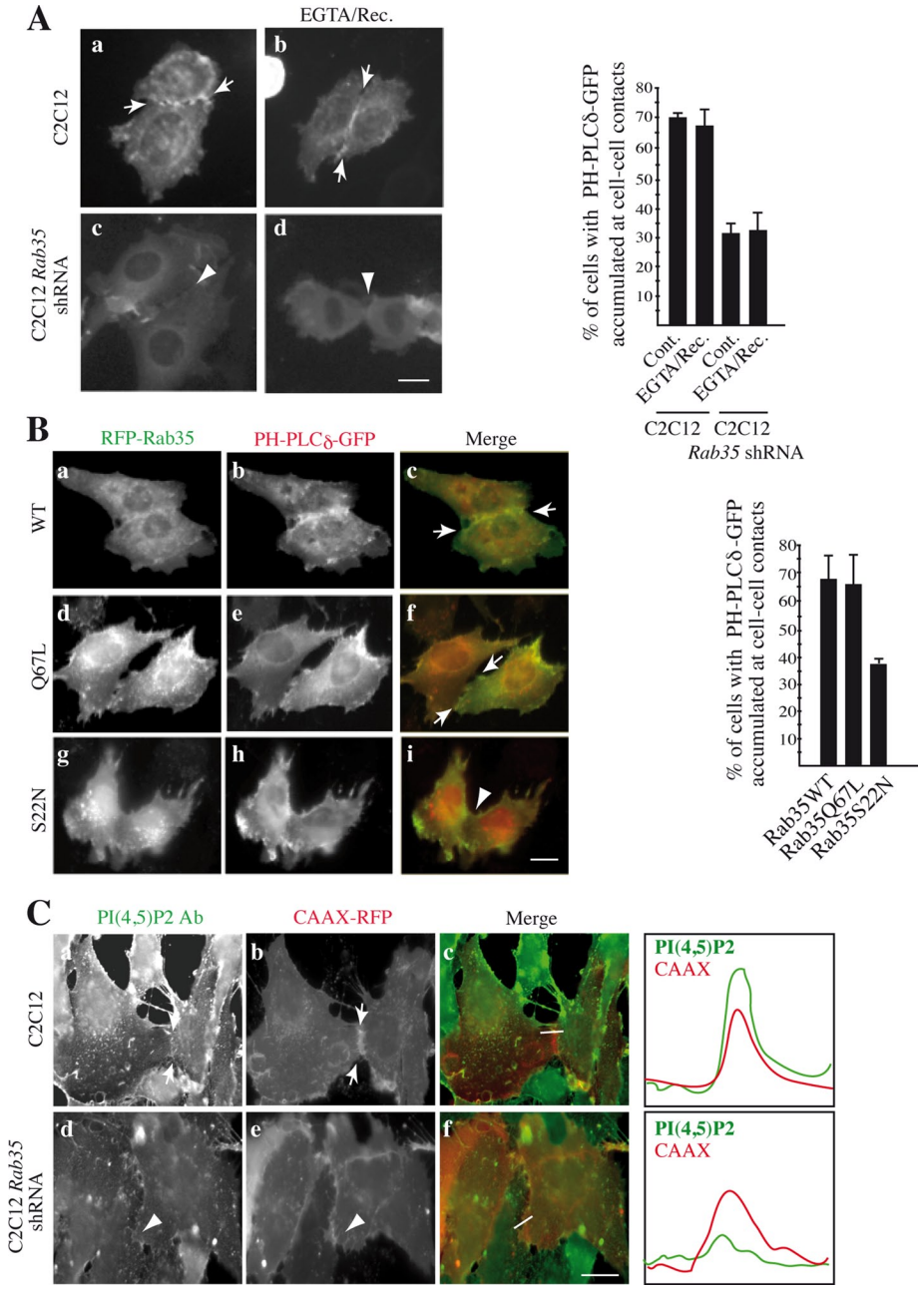

FIGURE 4: $PI(4,5)P_2$ accumulation at cell–cell contacts is reduced in *Rab35*-knockdown myoblasts. (A) Parental and *Rab35* shRNA C2C12 myoblasts were transfected with PH-PLCδ-GFP and left either untreated (a and c) or treated with EGTA for 20 min and then incubated in Ca^{2+}-containing medium for 60 min (EGTA/Rec., b and d). Arrows show accumulation and arrowheads show absence of accumulation of PH-PLCδ-GFP at cell contact sites. Bar, 10 μm. The histogram represents the percentage of cells in which PH-PLCδ-GFP accumulated at cell–cell contacts. At least three independent experiments were analyzed and 50 cells counted for each experiment. (B) C2C12 myoblasts were cotransfected with PH-PLCδ-GFP and RFP-fused Rab35WT (a–c), Rab35Q67L (d–f), or Rab35S22N (g–i). Arrows show Rab35 and PH-PLCδ-GFP accumulation, and arrowheads show absence of accumulation at cell contact sites. Bar, 10 μm. The histogram represents the proportion of cells in which PH-PLCδ-GFP accumulated at cell contact sites. At least three independent experiments were analyzed. Fifty cells were counted for each experiment. (C) Parental and *Rab35* shRNA C2C12 myoblasts were transfected with the RFP-fused CAAX construct (b and e) and stained using an anti-$PI(4,5)P_2$ antibody (a and d). Arrows show $PI(4,5)P_2$ and CAAX-RFP accumulation and arrowheads show absence of accumulation at cell contact sites. Bar, 10 μm. Quantification of the two signals was performed along the white line shown in the merge panels (c and f) by line scan (MetaMorph software).

accurate quantification of $PI(4,5)P_2$ at cell–cell contacts, we expressed red fluorescent protein (RFP) fused to a CAAX sequence that addresses RFP to the PM to normalize the signal given by the anti-$PI(4,5)P_2$ antibody. Line-scan analysis confirmed the decrease of $PI(4,5)P_2$ expression at cell–cell contacts in Rab35-depleted cells (representative line scan shown in Figure 4C).

These data show that Rab35 is required for $PI(4,5)P_2$ accumulation at cell–cell contacts.

$PI(4,5)P_2$ is required for cadherin accumulation at cell–cell contacts

$PI(4,5)P_2$, N- and M-cadherin (Taulet *et al.*, 2009; Bach *et al.*, 2010), and Rab35 (this study) accumulate at cell contacts in C2C12 myoblasts. Moreover, recruitment and activation of PIP5Kγ at sites of N-cadherin ligation, resulting in $PI(4,5)P_2$ production, have been reported (El Sayegh *et al.*, 2007). We thus asked whether $PI(4,5)P_2$ was required for N- and M-cadherin accumulation at cell–cell contacts. To decrease $PI(4,5)P_2$ level in cultured myoblasts, cells were treated with agents that reduce (calcimycin, LiCl) or mask (neomycin) $PI(4,5)P_2$ (Griffin and Hawthorne, 1978; Hallcher and Sherman, 1980; Gabev *et al.*, 1989; Laux *et al.*, 2000). Whereas in control cells, N- and M-cadherin accumulated at cell–cell contacts (Figure 5A, a and e, arrows), treatments that perturbed $PI(4,5)P_2$ disrupted cadherin accumulation at cell–cell contacts (Figure 5A, b–d and f–h, arrowheads). We then analyzed the effect of $PI(4,5)P_2$ reduction on N- and M-cadherin localization by using stable C2C12 cell lines in which *PIP5Kγ* expression was silenced by RNA interference (El Sayegh *et al.*, 2007; Ling *et al.*, 2007; Bach *et al.*, 2010). Moreover, $PI(4,5)P_2$ expression at cell–cell contacts was significantly lower in *PIP5Kγ* shRNA myoblasts than in control cells (Figure 5B). Both N- and M-cadherin accumulation at cell–cell contacts was perturbed in *PIP5Kγ* shRNA myoblasts (Figure 5C, d–f) in comparison to control *Luci* shRNA C2C12 cells (Figure 5C, a–c). Similarly, Rab35 was not recruited to cell–cell contacts in *PIP5Kγ* shRNA myoblasts compared with control *Luci* shRNA C2C12 myoblasts (Supplemental Figure S6). This is in agreement with our data showing that cadherins recruit Rab35 to cell–cell contact sites (Figure 1C). Moreover, whereas the level of p120 catenin was not modified in *PIP5Kγ* shRNA C2C12 myoblasts (Figure 5Da), p120 catenin association with N-cadherin (Figure 5Db) and M-cadherin (Figure 5Dc) was decreased. Conversely, β-catenin binding was not

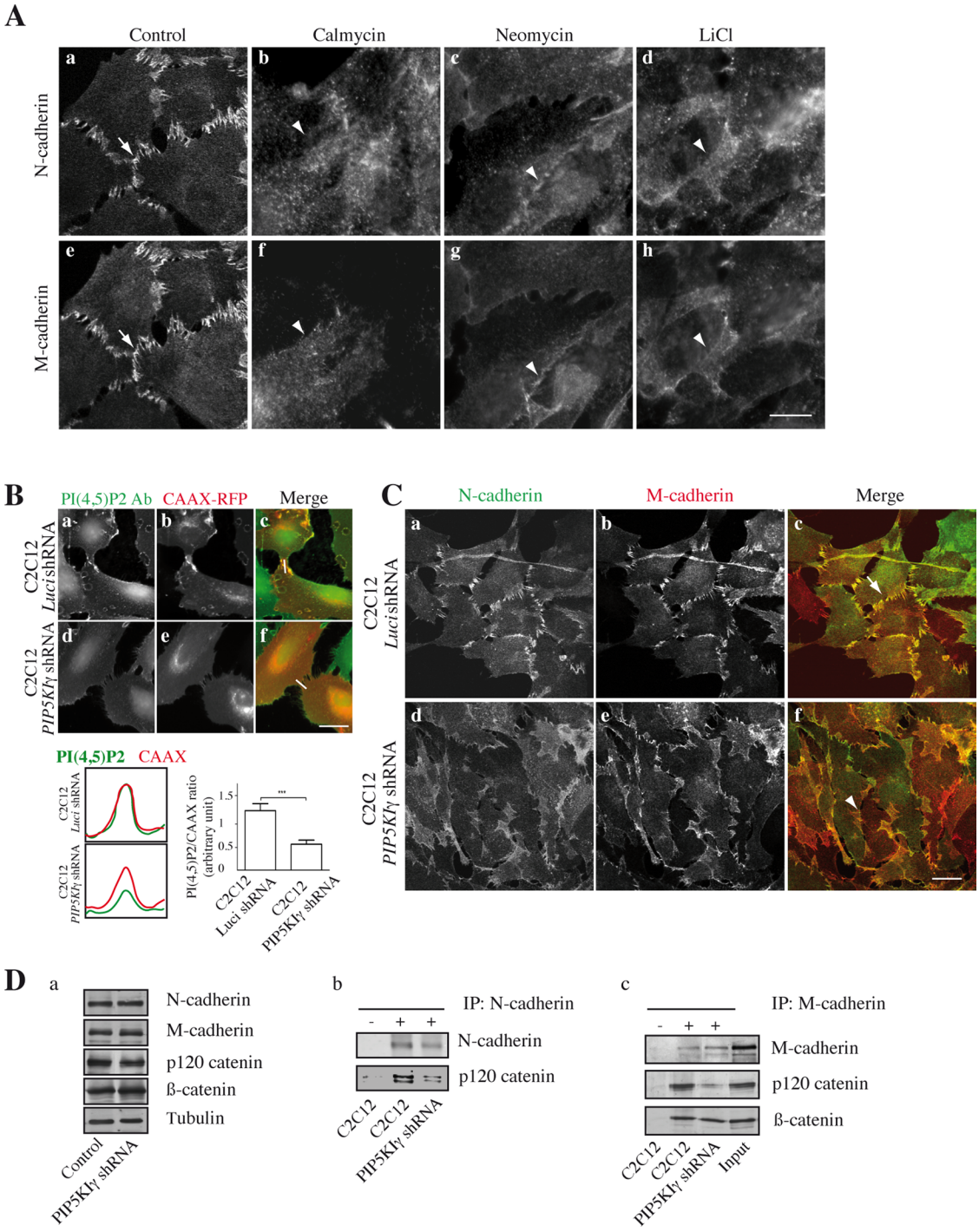

FIGURE 5: PI(4,5)P_2 accumulation at cell–cell contacts is required for N- and M-cadherin localization at cell contact sites. (A) C2C12 myoblasts were cultured in GM supplemented with agents that reduce (50 µM calcimycin or 1 mM LiCl) or mask (1 mM neomycin) PI(4,5)P_2, and after 16 h, N- and M-cadherin localization was analyzed by indirect immunofluorescence. Arrows show cadherin accumulation at cell contact sites, and arrowheads show absence of cadherin accumulation at cell contact sites. Bar, 10 µm. (B) Control *Luci* shRNA (a–c) and *PIP5KIγ* shRNA C2C12 myoblasts (d–f) were transfected with the RFP-fused CAAX construct and stained using an anti-PI(4,5)P_2 antibody. Bar, 10 µm. Quantification of the two signals was performed along the white line shown in the "merge" panels by line scan (MetaMorph software). The PI(4,5)P_2/CAAX ratio was quantified in 50 cells. (C) N- and M-cadherin localization was analyzed by indirect immunofluorescence in control *Luci* shRNA (a–c) and *PIP5KIγ* shRNA C2C12 myoblasts (d–f). Arrows show cadherin accumulation at cell contact sites, and arrowheads show perturbation of cadherin accumulation at cell contact sites. Bar, 10 µm. (D) a, Expression of N- and M-cadherin, p120 and β-catenins, and α-tubulin was analyzed by Western blotting in cell lysates of control *Luci* shRNA and *PIP5KIγ* shRNA C2C12 myoblasts. b, c, Cell lysates of *Luci* shRNA and *PIP5KIγ* shRNA C2C12 myoblasts were immunoprecipitated using anti–N-cadherin (b) or anti–M-cadherin (c) antibodies and probed for the presence of β- and p120 catenins. (–) Control immunoprecipitations were always performed using irrelevant immunoglobulins G.

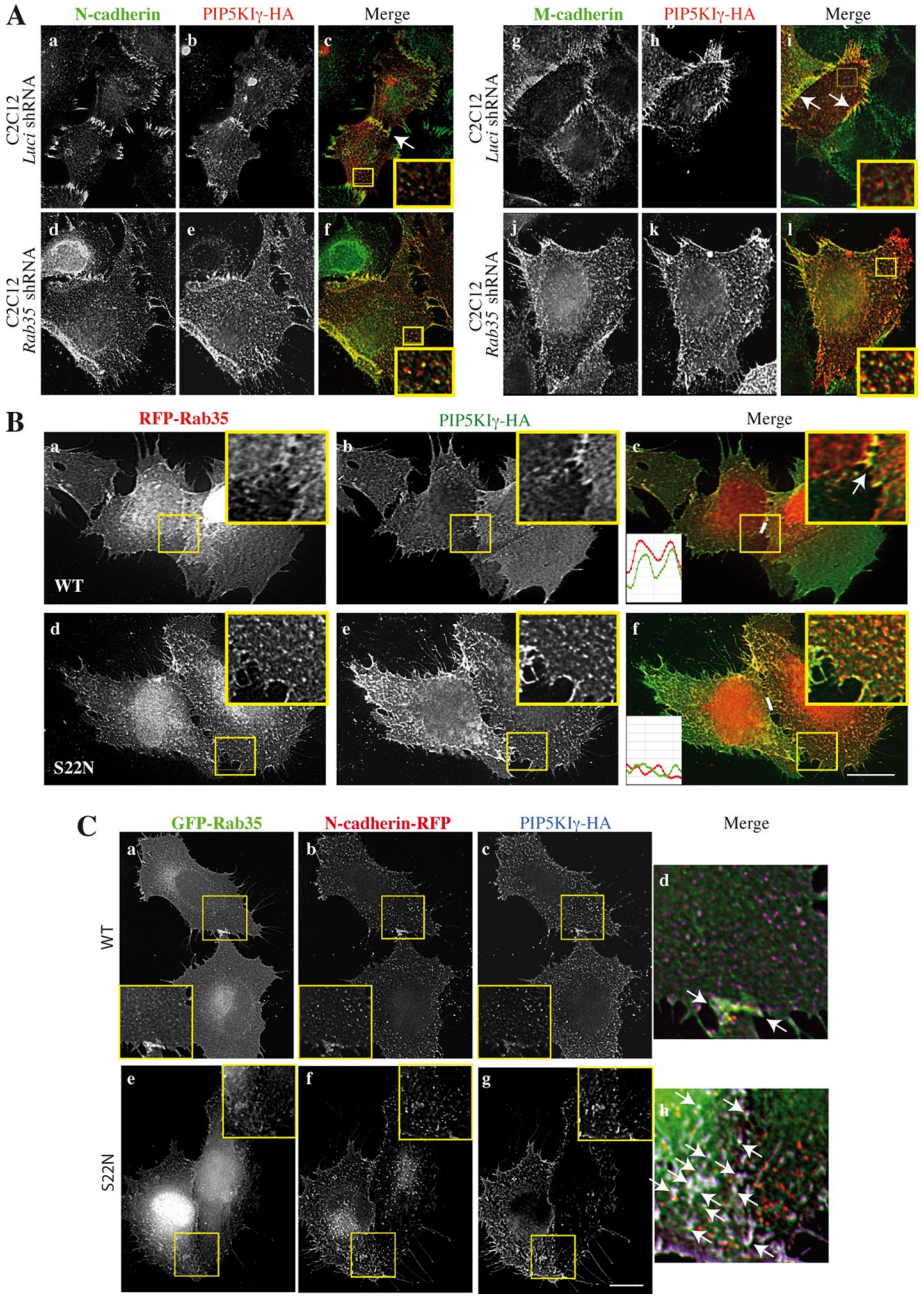

FIGURE 6: Rab35 is required for PIP5KIg accumulation at cell–cell contacts. (A) Control *Luci* shRNA (a–c and g–i) and *Rab35* shRNA C2C12 myoblasts (d–f and j–l) were transfected with HA-tagged PIP5KI γ and stained for N-cadherin (a–f) or M-cadherin (g–l) and for HA tag detection. Images were acquired using a wide-field microscope and deconvolved using the Huygens system image restoration software. Insets show enlarged selected areas. Arrows show colocalization of cadherins and PIP5KIγ at cell–cell contacts. Bar, 10 μm. (B) C2C12 myoblasts were transfected with HA-tagged PIP5KIγ and RFP-Rab35WT (a–c) or RFP-Rab35S22N (d–f) and stained for HA-tag detection. Images were acquired using a wide-field microscope and deconvolved using the Huygens system image restoration software. Insets show enlarged selected areas. Arrow shows colocalization of Rab35WT and PIP5KIγ at cell–cell contacts. Quantification of the two signals was performed along the white line shown in the "merge" panels by line scan (MetaMorph software; c and f). Bar, 10 μm. (C) C2C12 myoblasts were transfected with N-cadherin–RFP, HA-tagged PIP5KIγ, and GFP-Rab35WT (a–d) or RFP-Rab35S22N (e–h) and stained for HA-tag detection. Images were acquired using a wide-field microscope and deconvolved using the Huygens system image restoration software. Insets show enlarged selected areas; merge panels show colocalization of the three proteins in the selected areas. Arrow shows colocalization of N-cadherin, Rab35WT, and PIP5KIγ at cell–cell contacts or N-cadherin, Rab35S22N, and PIP5KIγ in clusters outside cell–cell contacts (d and h). Bar, 10 μm.

affected. The weak association of N- and M-cadherin with p120 catenin when $PI(4,5)P_2$ is reduced reflects an unstable cadherin complex at cell junctions.

Finally, we analyzed PIP5KIγ localization in *Rab35*-knockdown cells. PIP5KIγ accumulated at cell–cell contacts in control cells, where it colocalized with N- and M-cadherin (Figure 6A, a–c and g–i, arrows). In contrast, in *Rab35* shRNA C2C12 myoblasts, PIP5KIγ was no longer accumulated at cell–cell contacts, whereas its punctuated intracellular localization increased (Figure 6A, d–f and j–l). To analyze in more detail PIP5KIγ distribution, we cotransfected C2C12 myoblasts with hemagglutinin (HA)-tagged PIP5KIγ and either RFP-Rab35WT or RFP-Rab35S22N. PIP5K*I*γ was mostly found at the PM and accumulated at cell–cell contacts when coexpressed with Rab35WT (Figure 6B, a–c). Conversely, it colocalized with Rab35S22N in clusters located outside cell–cell contacts (Figure 6B, d–f). Moreover, N-cadherin was also found in these clusters with PIP5K*I*γ and Rab35S22N (Figure 6C). Taken together, these data show that 1) Rab35 is required for *PIP5KI*γ accumulation at cell–cell contacts and 2) $PI(4,5)P_2$ generated at cell–cell contacts is required for cadherin-dependent intercellular junction formation.

Rab35 knockdown inhibits myoblast differentiation

To analyze the functional consequence of *Rab35* knockdown, and because N- and M-cadherins are two major regulators of myogenesis induction and myoblast fusion (Charrasse *et al.*, 2002, 2006), we asked whether *Rab35* knockdown impaired myogenesis. First, C2C12 cells were grown to 80% confluency in growth medium (GM) and then shifted to differentiation medium (DM) for 4 d. Rab35 expression level increased during the differentiation process (Figure 7A). Then parental, *Luci* shRNA, and *Rab35* shRNA C2C12 myoblasts were induced to differentiate, and the expression of myogenin, troponin T, and myosin heavy chain (three myogenic markers) and myotube formation were analyzed. We observed a little decrease in the expression of these myogenic markers in *Rab35* shRNA myoblasts (Figure 7B). These results were confirmed using four different *Rab35* shRNA clones (*Rab35* shRNA1 A1 and A7; *Rab35* shRNA2 A1 and A10, unpublished data). Analysis of myogenin and troponin T expression by immunofluorescence after 2 d in DM also confirmed these results (unpublished data). In addition, time-lapse imaging of parental and *Rab35* shRNA myoblasts

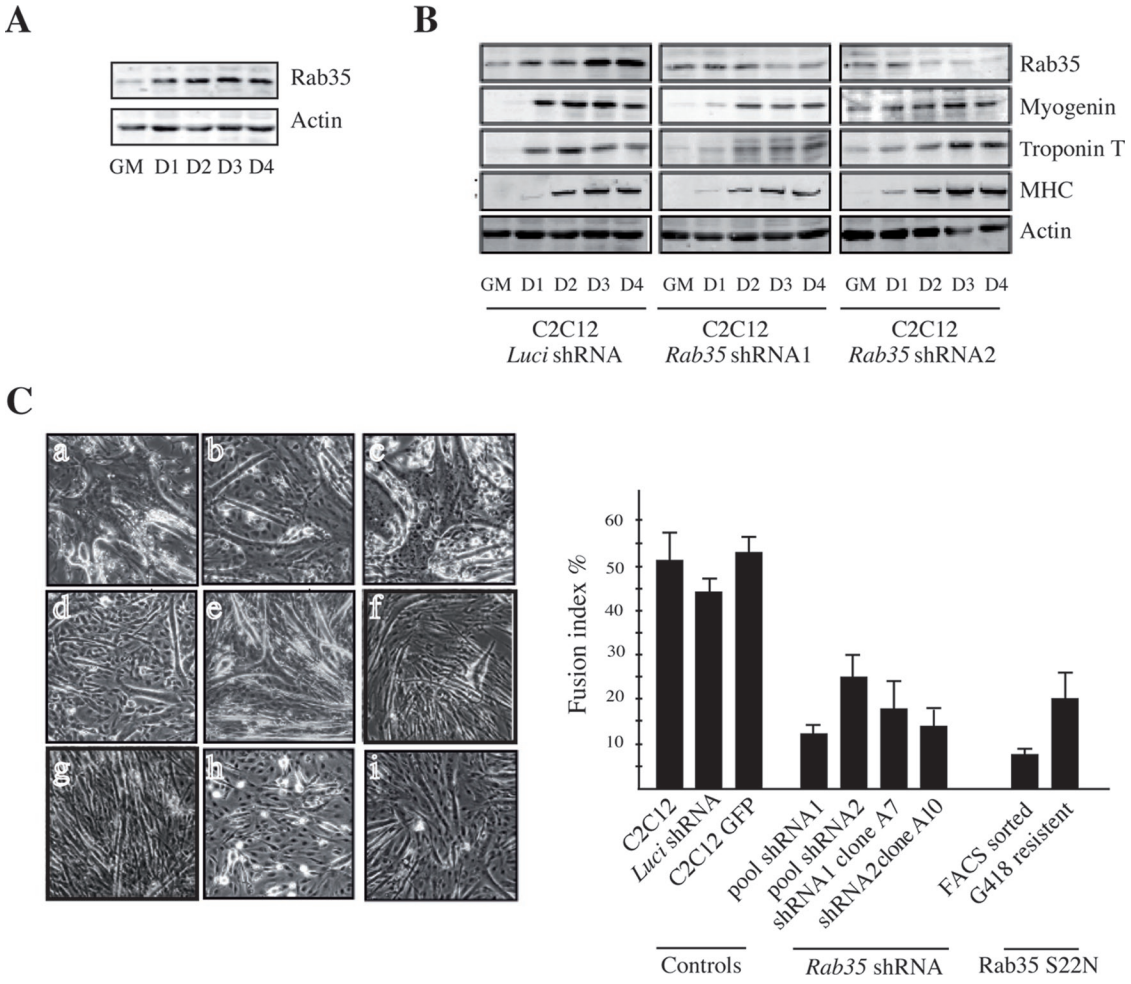

FIGURE 7: Inhibition of Rab35 expression by RNA interference affects myogenesis and myotube formation. (A) Protein extracts (50 µg/well) from C2C12 myoblasts, collected at the indicated time points (GM, growth medium; D, days after switching to differentiation medium, DM) were immunoblotted for assessing Rab35 and actin expression. (B) Cell lysates (30 µg) of *Luci* shRNA (control) and *Rab35* shRNA C2C12 myoblasts cultured in GM or DM for the indicated time were assessed by Western blot analysis for expression of Rab35, myogenin, troponin T, MHC, and actin. Results are representative of three independent experiments using cells that express Rab35 ShRNA1 or 2. (C) Phase contrast images of parental C2C12 (a), *Luci* shRNA C2C12 (b), GFP-expressing (vector alone) C2C12 cells sorted by FACS (c), *Rab35* shRNA C2C12 pools (d, shRNA1; e, shRNA2) and clones (f, shRNA1 clone A7; g, shRNA2 clone A10), and GFP-Rab35S22N–expressing C2C12 myoblasts (h, sorted by FACS; i, selected by G418 resistance) 4 d after DM addition. Bar, 30 µm. The histogram represents the fusion index in control myoblasts, the indicated *Rab35* shRNA pools and clones, and C2C12 myoblasts that express Rab35S22N. The results are representative of three independent experiments. At least 3000 nuclei were counted for each experiment.

revealed that *Rab35* silencing perturbed myoblast fusion (Supplemental Video S5; left, parental C2C12 cells; right, *Rab35* shRNA2 myoblasts). A significant reduction in the number of myotubes and in the fusion index was observed in *Rab35* shRNA myoblasts after 4 d in DM (Figure 7C, d–g) in comparison to controls (Figure 7C, a–c). Comparable results were obtained with the different *Rab35* shRNA clones and pooled cells. Moreover, these findings were confirmed using C2C12 myoblasts that express the dominant-negative mutant Rab35S22N-GFP after selection by fluorescence-activated cell sorting (FACS) or with a resistance marker (G418; (Figure 7C, h and i). These data show that Rab35 is required for myogenesis and more specifically for myotube formation and fusion.

DISCUSSION

AJs are very dynamic structures, and their continuous remodeling is vital for the maintenance of tissue integrity, morphogenetic movements, delamination, and epithelial-to-mesenchymal transition (Harris and Tepass, 2011). Here we report that the Rab35 GTPase is a new regulator of cadherin-dependent AJ formation through regulation of cadherin trafficking and stabilization at cell–cell contacts.

Endocytosed cadherins can undergo multiple fates, including degradation or recycling back to the PM. In Rab35-depleted cells, cadherin localization at the cell surface was reduced (Figure 3D), whereas their total level was not decreased, suggesting that Rab35 regulates the recycling of internalized cadherins. Previous studies linked Rab35 to the recycling pathways from endosomes to the PM of cargoes that are internalized in a clathrin-dependent or clathrin-independent way, such as transferrin or MHCI (Kouranti *et al.*, 2006; Patino-Lopez *et al.*, 2008; Allaire *et al.*, 2010). This suggests that clathrin-dependent and clathrin-independent cargoes could use common machineries for recycling back to the cell surface from recycling endosomes. This is consistent with the fact that cadherins

undergo endocytic processing through several internalization routes from the PM (Delva and Kowalczyk, 2009; Schill and Anderson, 2009; Harris and Tepass, 2011). Rab35 does not generally control the recycling of all transmembrane proteins but allows selective recycling of some cargoes from early endosomes. Indeed, it was previously demonstrated that Rab35 controls recycling of MHCI (Allaire *et al.*, 2010; Chesneau *et al.*, 2012) but not of β1-integrin from early endosomes (Allaire *et al.*, 2010). Until now, only few cargoes that require Rab35 for their recycling had been identified, and here we demonstrate that cadherins are among them.

To characterize the compartments in which cadherins are located after *Rab35* depletion, various GFP-tagged Rab family members were expressed, such as Rab4, 5, 7, 8, and 11. With the exception of Rab5, none of the tested Rab members localized in the compartment in which cadherins accumulated. We observed an enlargement of Rab5-positive early endosomes, as described (Allaire *et al.*, 2010). A clear colocalization upon Rab35 depletion between cadherins and transferrin was detected (Figure 3D). This is consistent with studies linking Rab35 to the recycling of transferrin back to the PM (Kouranti *et al.*, 2006; Patino-Lopez *et al.*, 2008; Chesneau *et al.*, 2012). Finally, we demonstrate that cadherins and clathrin heavy chain or AP-2 colocalize in cells that express dominant-negative Rab35. This is not surprising because Rab35 and connecdenn, a GEF for Rab35, are both expressed in clathrin-coated vesicles (Allaire *et al.*, 2010).

Besides its role in cadherin localization at the PM, Rab35 could also affect cadherin stabilization at cell–cell contacts through a decrease of $PI(4,5)P_2$ production at cell–cell contact sites. We confirm here, as previously shown in epithelial cells (Ling *et al.*, 2007), that the production of $PI(4,5)P_2$ at cell–cell contact sites is important for cadherin stability. Recruitment and activation of PIP5KIγ at sites of N- and E-cadherin ligation result in $PI(4,5)P_2$ production (Akiyama *et al.*, 2005; El Sayegh *et al.*, 2007; Ling *et al.*, 2007). PIP5KIγ interacts directly with the cytoplasmic tail of cadherins and is required for E-cadherin–mediated AJ assembly. Moreover, expression of a kinase-inactive form of PIP5KIγ showed that $PI(4,5)P_2$ generation is required for AJ assembly (Ling *et al.*, 2007) and local actin assembly at AJs (El Sayegh *et al.*, 2007). When Rab35 is inhibited, PIP5KIγ is not accumulated at cell–cell contacts and is sequestered in membrane vesicles with cadherins and Rab35. The colocalization of PIP5KIγ with cadherins in these structures is not surprising, because cadherin and PIP5KIγ are associated (El Sayegh *et al.*, 2007) and are relocated to similar intracellular areas when cell–cell contacts are disrupted upon reduction of calcium ion concentration (Ling *et al.*, 2007). As a consequence, $PI(4,5)P_2$ production at cell–cell contacts is impaired. These results argue for a role of Rab35 in the control of cadherins and PIP5KIγ localization at cell–cell contacts. In stable C2C12 cell lines in which *PIP5KIγ* expression was silenced by RNA interference we observed 1) a decrease in the amount of $PI(4,5)P_2$ at cell–cell contacts (Figure 5B) and 2) perturbation of N- and M-cadherin accumulation at cell–cell contacts (Figure 5C). The perturbation of N- and M-cadherin accumulation at cell–cell contacts in *PIP5KIγ* shRNA myoblasts is always less pronounced than in *Rab35* shRNA myoblasts. This indicates that inhibition of PIP5Kγ affects only $PI(4,5)P_2$ production at cell–cell contacts, which then perturbs cadherin stabilization. Conversely, inhibition of Rab35 affects both cadherin and PIP5K delivery to the plasma membrane and thus has a more pronounced effect on cadherin accumulation at cell–cell contacts. Indeed, in addition to the inhibition of PIP5K and $PI(4,5)P_2$ production at cell–cell contacts, which impairs cadherin stabilization, Rab35 inhibition also blocks cadherin delivery into vesicles/clusters outside cell–cell contacts.

Functionally, we found that Rab35 is required for myoblast fusion to occur and observed that Rab35 expression level increased during myoblast fusion. Until now the only Rab involved in myoblast fusion was Rab11 in *Drosophila* (Bhuin and Roy, 2009). The defect in myoblast fusion we observed in C2C12 myoblasts in which *Rab35* was silenced could be explained by the decrease of cadherin accumulation and $PI(4,5)P_2$ production at cell–cell contacts. Indeed, myoblast fusion is characterized by $PI(4,5)P_2$ accumulation at cell–cell contact sites (Bach *et al.*, 2010). $PI(4,5)P_2$ decrease at contact sites might thus impair the recruitment at fusion sites of PH domain–containing proteins involved in the regulation of myoblast fusion, such as Trio, Rac1, and Arf6, through the reorganization of the actin cytoskeleton and of PM dynamics (Macia *et al.*, 2008). Moreover, Rab35 could participate in the control of myoblast fusion through the regulation of EHD1, one of the four carboxyl-terminal Eps15 homology domain-containing (EHD) proteins. Indeed, EHD proteins have a role in endocytic regulation and have been linked to several Rab family members through their association with mutual effectors (Naslavsky and Caplan, 2011). Of interest, Rab35 controls early endosomal recruitment of EHD1 (Allaire *et al.*, 2010), a protein that was recently shown to be involved in myoblast fusion (Posey *et al.*, 2011).

In conclusion, we report here that Rab35 controls cadherin-mediated AJ formation and myoblast fusion. Given that Rab35 regulates cadherin function, it will now be interesting to investigate whether dysfunction of Rab35 might be associated with cancer development or with skeletal muscle pathologies such as muscular dystrophies.

MATERIALS AND METHODS

Cell culture

HeLa cells were cultured in DMEM supplemented with 10% fetal bovine serum. Culture and differentiation of C2C12 mouse myoblasts were done as described (Charrasse *et al.*, 2006). *PIP5KIγ* shRNA C2C12myoblasts were described previously (Bach *et al.*, 2010).

EGTA was used at 2 mM for 1 h, and then cells were rinsed in GM for 1 h. Calcimycin (50 µM; Sigma-Aldrich, St. Louis, MO), LiCl (1 mM; Sigma-Aldrich), and neomycin (1 mM; Sigma-Aldrich) were added to GM for 16 h.

DNA constructs and RNA interference

shRNA constructs were made using the retroviral vector pSIREN-RetroQ according to the manufacturer's protocol (BD Biosciences, San Diego, CA). To suppress endogenous *Rab35* expression, the annealed double-strand oligonucleotides GATCCG**gacaacttggcgaaacagc**TTCAAGAGA**gctgtttcgccaagttgtc**CTTTTTTACGCGTG (top) and AATTCACGCGTAAAAAAG**gacaacttggcgaaacagc**TCTCTTGAA**gctgtttcgccaagttgtc**CG (bottom) were inserted into the RNAi-Ready pSIREN-RetroQ vector (Clontech, Mountain View, CA) to produce *Rab35* shRNA1. Bold letters correspond to oligonucleotides 680–688 of the mouse *Rab35* cDNA sequence (NM-198163). For *Rab35* shRNA2, the sequence in bold letters of the top strand of the shRNA1 was replaced by GATCCG**ccttctcaggcagctacat**TTCAAGAGA**atgtagctgcctgagaagg**CTTTTTTACGCGTG (oligonucleotides 255–273 of the *Rab35* sequence). Luciferase shRNA was used as control (Fortier *et al.*, 2008). Retrovirus production in Phoenix cells, infection, and selection were performed as described (Fortier *et al.*, 2008). Cells were grown continuously in 1 µg/ml puromycin. Different clones were isolated by limited dilution. *Rab35* silencing was assessed in 11 random clones and a pool of *Rab35* shRNA1 pSIREN-RetroQ C2C12 myoblasts and in 10 random clones and a pool of *Rab35* shRNA2 pSIREN-RetroQ C2C12 myoblasts.

All presented experiments were performed with at least the pool and two random clones in triplicate.

Gel electrophoresis and immunoblotting

Cells cultured in 100-mm dishes were rinsed in cold phosphate-buffered saline (PBS) and lysed in 10 mM piperazine-*N*,*N*′-bis(2-ethanesulfonic acid), pH 7.0, 100 mM NaCl, 300 mM sucrose, 3 mM MgCl2, 0.5% NP40, 1 mM EDTA, 1 mM orthovanadate, and protease inhibitor cocktail (Sigma-Aldrich). Then 30- to 50-μg protein extracts were resolved on polyacrylamide gels (8, 12, and 15%) and transferred onto Immobilon-FL membranes. Membranes were incubated with monoclonal antibodies against N-cadherin (1:1000), β-catenin (1:500), p120 catenin (1:1000), and Rab11 (1:1000; BD Transduction Laboratories, Lexington, KY), troponin T (1:500), α-tubulin (1:500), and myosin (1:2000; Sigma-Aldrich), fascin (1:500; Abcam, Cambridge, MA), and M-cadherin (1:200; NanoTools, Munich, Germany) or with polyclonal antibodies against Rab35 (1:800; gift from A. Echard), myogenin (Santa Cruz Biotechnology, Santa Cruz, CA), GFP (1:800; Rockland Immunochemicals, Gilbertsville, PA), and actin (1:1000; Sigma-Aldrich). After washing, membranes were incubated with IRDye^{R} 680 or 800 secondary antibodies (LI-COR Biosciences, Lincoln, NE). Detection and analysis were performed using the Odyssey Infrared imaging system (LI-COR Biosciences). Quantification analysis of Western blots was performed by densitometry using Odyssey, version 3.0, and ImageJ (National Institutes of Health, Bethesda, MD).

Immunoprecipitation

Cell lysates were obtained as described. Monoclonal anti–N- or M-cadherin antibodies or irrelevant monoclonal antibody (1 μg) were incubated with protein G (Dynabeads; Invitrogen, Carlsbad, CA) at room temperature for 30 min. After washing, 1 mg of protein extract was added at room temperature for 1 h.

Cell surface biotinylation

The presence of N- and M-cadherin at the cell surface was analyzed as described previously (Charrasse *et al*., 2006). Quantification of at least three independent experiments was performed using the Odyssey system.

Immunofluorescence and image acquisition

Cells were transfected with plasmids encoding HA-, GFP-, or RFP-tagged Rab35WT, Rab35Q67L, or Rab35S22N (from Genaro Patino-Lopez, National Institutes of Health/National Cancer Institute) or N-cadherin, M-cadherin, PH-PLCγ, PIP5KIγ, CAAX, Rab4WT, Rab5WT, Rab7WT, Rab8WT, or Rab11WT using JetPEI (Polyplus-transfection SA, Illkirch, France) and then fixed in 3.2% paraformaldehyde in PBS for 15 min. After 5-min permeabilization with 0.1% Triton X-100 in PBS, cells were incubated with mouse monoclonal anti-HA (1:2000), monoclonal anti–N-cadherin (1:200), anti–E-cadherin (1:1000), anti–clathrin heavy chain (1:100) and anti–adaptin-α (AP-2, 1:100; all from BD Transduction Laboratories) or affinity-purified anti–M-cadherin and N-cadherin (1:50) antibodies. Antibodies were revealed with Alexa Fluor 546–conjugated, Alexa Fluor 488–conjugated, or Alexa Fluor 633–conjugated goat anti–mouse or rabbit antibodies (Molecular Probes, Eugene, OR).

For transferrin uptake, cells were incubated in DMEM at 37°C for 30 min. Tetramethyl-rhodamine–labeled transferrin (20 μg/ml in medium containing 1% BSA; Molecular Probes) was internalized at 37°C for 45 min to reach the turnover steady state, and then cells were rinsed twice before fixation and cadherin expression analysis by immunofluorescence. For PI(4,5)P_2 detection, an anti-PI(4,5)P_2 monoclonal antibody (2C11; Santa Cruz Biotechnology) was used according to the protocol described in Hammond *et al*. (2009).

Images were taken either with a Zeiss LSM Meta 510 confocal microscope or with a MetaMorph-driven (Molecular Devices, Sunnyvale, CA) wide-field Axioimager Z2 fluorescence microscope (Zeiss, Jena, Germany) with a PL APO 63× objective (numerical aperture 1.32; Leica, Melville, NY) and a CoolSNAP HQ camera (Photometrics, Woburn, MA). Images were processed using Photoshop and Illustrator (Adobe, San Jose, CA).

Deconvolution

Sixteen-bit images were captured and epifluorescence images were first restored with Huygens (Scientific Volume Imaging, Hilversum, Netherlands; Ponti *et al*., 2007). Huygens is an iterative program that can reassign light, after encoding as gray levels, to its sources in the stack with a very high probability using a point spread function. This process removes the fuzziness contained in the stack while keeping the three-dimensional information. In the present study the maximum likelihood estimation algorithm was used throughout. Restored stacks were then further processed with Imaris (Bitplane, Zurich, Switzerland). Colocalization was analyzed with the Imaris Colocalization module.

Time-lapse experiments

Parental and *Rab35* shRNA C2C12 myoblasts were grown to confluence before analysis by time-lapse microscopy. Alternatively, parental and *Rab35* shRNA C2C12 myoblasts were transfected with N-cadherin–GFP/RFP, M-cadherin–GFP, Rab35WT-RFP, or Rab35S22N-RFP. Time-lapse confocal microscopy was performed using a spinning Nipkow disk. Images were saved as .tif files and further compiled into QuickTime movies (Apple, Cupertino, CA) using the MetaMorph program.

ACKNOWLEDGMENTS

We are grateful to Genaro Patino-Lopez (National Institutes of Health) for providing various plasmids encoding the RFP- and GFP-tagged Rab35 constructs. We thank the Montpellier RIO Imaging Facility. This work was supported by the Ligue Nationale contre le Cancer (Equipe labellisée), the Institut National du Cancer, and the Association Française contre les Myopathies. C.G.R. was supported by the Institut National de la Santé et de la Recherche Médicale. A.E. was supported by grants from the Institut Pasteur, the Center National de la Recherche Scientifique, and the Schlumberger Foundation for Education and Research.

REFERENCES

Akiyama C, Shinozaki-Narikawa N, Kitazawa T, Hamakubo T, Kodama T, Shibasaki Y (2005). Phosphatidylinositol-4-phosphate 5-kinase gamma is associated with cell-cell junction in A431 epithelial cells. Cell Biol Int 29, 514–520.

Allaire PD, Marat AL, Dall'Armi C, Di Paolo G, McPherson PS, Ritter B (2010). The Connecdenn DENN domain: a GEF for Rab35 mediating cargo-specific exit from early endosomes. Mol Cell 37, 370–382.

Bach AS, Enjalbert S, Comunale F, Bodin S, Vitale N, Charrasse S, Gauthier-Rouviere C (2010). ADP-ribosylation factor 6 regulates mammalian myoblast fusion through phospholipase D1 and phosphatidylinositol 4,5-bisphosphate signaling pathways. Mol Biol Cell 21, 2412–2424.

Baum B, Georgiou M (2011). Dynamics of adherens junctions in epithelial establishment, maintenance, and remodeling. J Cell Biol 192, 907–917.

Bhuin T, Roy JK (2009). Rab11 is required for myoblast fusion in *Drosophila*. Cell Tissue Res 336, 489–499.

Braga VM, Betson M, Li X, Lamarche-Vane N (2000). Activation of the small GTPase Rac is sufficient to disrupt cadherin-dependent cell-cell adhesion in normal human keratinocytes. Mol Biol Cell 11, 3703–3721.

Charrasse S, Comunale F, Grumbach Y, Poulat F, Blangy A, Gauthier-Rouviere C (2006). RhoA GTPase regulates M-cadherin activity and myoblast fusion. Mol Biol Cell 17, 749–759.
Charrasse S, Meriane M, Comunale F, Blangy A, Gauthier-Rouviere C (2002). N-cadherin-dependent cell-cell contact regulates Rho GTPases and beta-catenin localization in mouse C2C12 myoblasts. J Cell Biol 158, 953–965.
Chesneau L, Dambournet D, Machicoane M, Kouranti I, Fukuda M, Goud B, Echard A (2012). An ARF6/Rab35 GTPase cascade for endocytic recycling and successful cytokinesis. Curr Biol 22, 147–153.
Chevallier J, Koop C, Srivastava A, Petrie RJ, Lamarche-Vane N, Presley JF (2009). Rab35 regulates neurite outgrowth and cell shape. FEBS Lett 583, 1096–1101.
Christofori G (2003). Changing neighbours, changing behaviour: cell adhesion molecule-mediated signalling during tumour progression. EMBO J 22, 2318–2323.
Dambournet D, Machicoane M, Chesneau L, Sachse M, Rocancourt M, El Marjou A, Formstecher E, Salomon R, Goud B, Echard A (2011). Rab35 GTPase and OCRL phosphatase remodel lipids and F-actin for successful cytokinesis. Nat Cell Biol 13, 981–988.
Davis MA, Ireton RC, Reynolds AB (2003). A core function for p120-catenin in cadherin turnover. J Cell Biol 163, 525–534.
Delva E, Kowalczyk AP (2009). Regulation of cadherin trafficking. Traffic 10, 259–267.
Desclozeaux M, Venturato J, Wylie FG, Kay JG, Joseph SR, Le HT, Stow JL (2008). Active Rab11 and functional recycling endosome are required for E-cadherin trafficking and lumen formation during epithelial morphogenesis. Am J Physiol Cell Physiol 295, C545–556.
Egami Y, Fukuda M, Araki N (2011). Rab35 regulates phagosome formation through recruitment of ACAP2 in macrophages during FcgammaR-mediated phagocytosis. J Cell Sci 124, 3557–3567.
El Sayegh TY, Arora PD, Ling K, Laschinger C, Janmey PA, Anderson RA, McCulloch CA (2007). Phosphatidylinositol-4,5 bisphosphate produced by PIP5KIgamma regulates gelsolin, actin assembly, and adhesion strength of N-cadherin junctions. Mol Biol Cell 18, 3026–3038.
Fortier M, Comunale F, Kucharczak J, Blangy A, Charrasse S, Gauthier-Rouviere C (2008). RhoE controls myoblast alignment prior fusion through RhoA and ROCK. Cell Death Differ 15, 1221–1231.
Fukata M, Kaibuchi K (2001). Rho-family GTPases in cadherin-mediated cell-cell adhesion. Nat Rev Mol Cell Biol 2, 887–897.
Gabev E, Kasianowicz J, Abbott T, McLaughlin S (1989). Binding of neomycin to phosphatidylinositol 4,5-bisphosphate (PIP2). Biochim Biophys Acta 979, 105–112.
Gao Y, Balut CM, Bailey MA, Patino-Lopez G, Shaw S, Devor DC (2010). Recycling of the Ca^{2+}-activated K^+ channel, KCa2.3, is dependent upon RME-1, Rab35/EPI64C, and an N-terminal domain. J Biol Chem 285, 17938–17953.
Griffin HD, Hawthorne JN (1978). Calcium-activated hydrolysis of phosphatidyl-myo-inositol 4-phosphate and phosphatidyl-myo-inositol 4,5-bisphosphate in guinea-pig synaptosomes. Biochem J 176, 541–552.
Halbleib JM, Nelson WJ (2006). Cadherins in development: cell adhesion, sorting, and tissue morphogenesis. Genes Dev 20, 3199–3214.
Hallcher LM, Sherman WR (1980). The effects of lithium ion and other agents on the activity of myo-inositol-1-phosphatase from bovine brain. J Biol Chem 255, 10896–10901.
Hammond GR, Schiavo G, Irvine RF (2009). Immunocytochemical techniques reveal multiple, distinct cellular pools of PtdIns4P and PtdIns(4,5)P(2). Biochem J 422, 23–35.
Harris TJ, Tepass U (2011). Adherens junctions: from molecules to morphogenesis. Nat Rev Mol Cell Biol 11, 502–514.
Kawauchi T, Sekine K, Shikanai M, Chihama K, Tomita K, Kubo K, Nakajima K, Nabeshima Y, Hoshino M (2010). Rab GTPases-dependent endocytic pathways regulate neuronal migration and maturation through N-cadherin trafficking. Neuron 67, 588–602.
Kemler R (1993). From cadherins to catenins: cytoplasmic protein interactions and regulation of cell adhesion. Trends Genet 9, 317–321.
Kobayashi H, Fukuda M (2012). Rab35 regulates Arf6 activity through centaurin-B2 (ACAP2) during neurite outgrowth. J Cell Sci 125, 2235–2243.
Kouranti I, Sachse M, Arouche N, Goud B, Echard A (2006). Rab35 regulates an endocytic recycling pathway essential for the terminal steps of cytokinesis. Curr Biol 16, 1719–1725.
Laux T, Fukami K, Thelen M, Golub T, Frey D, Caroni P (2000). GAP43, MARCKS, and CAP23 modulate PI(4,5)P(2) at plasmalemmal rafts, and regulate cell cortex actin dynamics through a common mechanism. J Cell Biol 149, 1455–1472.
Ling K, Bairstow SF, Carbonara C, Turbin DA, Huntsman DG, Anderson RA (2007). Type Igamma phosphatidylinositol phosphate kinase modulates adherens junction and E-cadherin trafficking via a direct interaction with mu 1B adaptin. J Cell Biol 176, 343–353.
Lozano E, Betson M, Braga VM (2003). Tumor progression: small GTPases and loss of cell-cell adhesion. Bioessays 25, 452–463.
Macia E, Partisani M, Favard C, Mortier E, Zimmermann P, Carlier MF, Gounon P, Luton F, Franco M (2008). The pleckstrin homology domain of the Arf6-specific exchange factor EFA6 localizes to the plasma membrane by interacting with phosphatidylinositol 4,5-bisphosphate and F-actin. J Biol Chem 283, 19836–19844.
Naslavsky N, Caplan S (2011). EHD proteins: key conductors of endocytic transport. Trends Cell Biol 21, 122–131.
Palacios F, Price L, Schweitzer J, Collard JG, D'Souza-Schorey C (2001). An essential role for ARF6-regulated membrane traffic in adherens junction turnover and epithelial cell migration. EMBO J 20, 4973–4986.
Palacios F, Tushir JS, Fujita Y, D'Souza-Schorey C (2005). Lysosomal targeting of E-cadherin: a unique mechanism for the down-regulation of cell-cell adhesion during epithelial to mesenchymal transitions. Mol Cell Biol 25, 389–402.
Patino-Lopez G, Dong X, Ben-Aissa K, Bernot KM, Itoh T, Fukuda M, Kruhlak MJ, Samelson LE, Shaw S (2008). Rab35 and its GAP EPI64C in T cells regulate receptor recycling and immunological synapse formation. J Biol Chem 283, 18323–18330.
Perez-Moreno M, Jamora C, Fuchs E (2003). Sticky business: orchestrating cellular signals at adherens junctions. Cell 112, 535–548.
Ponti A, Schward P, Gulati A, Bäcker V (2007). Huygens Remote Manager. Imaging Microsc 9, 57–58.
Posey ADJr, Pytel P, Gardikiotes K, Demonbreun AR, Rainey M, George M, Band H, McNally EM (2011). Endocytic recycling proteins EHD1 and EHD2 interact with fer-1-like-5 (Fer1L5) and mediate myoblast fusion. J Biol Chem 286, 7379–7388.
Rahajeng J, Panapakkam Giridharan SS, Cai B, Naslavsky N, Caplan S (2012). MICAL-L1 is a tubular endosomal membrane hub that connects Rab35 and Arf6 with Rab8a. Traffic 13, 82–93.
Roeth JF, Sawyer JK, Wilner DA, Peifer M (2009). Rab11 helps maintain apical crumbs and adherens junctions in the *Drosophila* embryonic ectoderm. PLoS One 4, e7634.
Schill NJ, Anderson RA (2009). Out, in and back again: PtdIns(4,5)P(2) regulates cadherin trafficking in epithelial morphogenesis. Biochem J 418, 247–260.
Shim J, Lee SM, Lee MS, Yoon J, Kweon HS, Kim YJ (2010). Rab35 mediates transport of Cdc42 and Rac1 to the plasma membrane during phagocytosis. Mol Cell Biol 30, 1421–1433.
Stenmark H (2009). Rab GTPases as coordinators of vesicle traffic. Nat Rev Mol Cell Biol 10, 513–525.
Takeichi M (1995). Morphogenetic roles of classic cadherins. Curr Opin Cell Biol 7, 619–627.
Taulet N, Comunale F, Favard C, Charrasse S, Bodin S, Gauthier-Rouviere C (2009). N-cadherin/p120 catenin association at cell-cell contacts occurs in cholesterol-rich membrane domains and is required for RhoA activation and myogenesis. J Biol Chem 284, 23137–23145.
Troyanovsky S (2005). Cadherin dimers in cell-cell adhesion. Eur J Cell Biol 84, 225–233.
Varnai P, Balla T (1998). Visualization of phosphoinositides that bind pleckstrin homology domains: calcium- and agonist-induced dynamic changes and relationship to myo-[3H]inositol-labeled phosphoinositide pools. J Cell Biol 143, 501–510.
Xiao K, Allison DF, Buckley KM, Kottke MD, Vincent PA, Faundez V, Kowalczyk AP (2003). Cellular levels of p120 catenin function as a set point for cadherin expression levels in microvascular endothelial cells. J Cell Biol 163, 535–545.
Yap AS, Crampton MS, Hardin J (2007). Making and breaking contacts: the cellular biology of cadherin regulation. Curr Opin Cell Biol 19, 508–514.
Zerial M, McBride H (2001). Rab proteins as membrane organizers. Nat Rev Mol Cell Biol 2, 107–117.
Zhang J, Fonovic M, Suyama K, Bogyo M, Scott MP (2009). Rab35 controls actin bundling by recruiting fascin as an effector protein. Science 325, 1250–1254.